MolecularMedicine

Gene Expression Analysis Reveals Inhibition of Radiation-Induced TGFβ-Signaling by Hyperbaric Oxygen Therapy in Mouse Salivary Glands

Linda Spiegelberg,[1] Sigrid MA Swagemakers,[2] Wilfred FJ van IJcken,[3] Edwin Oole,[3] Eppo B Wolvius,[1] Jeroen Essers,[4,5,6] Joanna AM Braks[1]

[1]Department of Oral and Maxillofacial Surgery, [2] Department of Bioinformatics, [3]Center for Biomics, [4]Department of Cell Biology and Genetics, Cancer Genomics Center, [5]Department of Radiation Oncology, and [6]Department of Vascular Surgery, Erasmus MC, Rotterdam, the Netherlands

A side effect of radiation therapy in the head and neck region is injury to surrounding healthy tissues such as irreversible impaired function of the salivary glands. Hyperbaric oxygen therapy (HBOT) is clinically used to treat radiation-induced damage but its mechanism of action is largely unknown. In this study, we investigated the molecular pathways that are affected by HBOT in mouse salivary glands two weeks after radiation therapy by microarray analysis. Interestingly, HBOT led to significant attenuation of the radiation-induced expression of a set of genes and upstream regulators that are involved in processes such as fibrosis and tissue regeneration. Our data suggest that the TGFβ-pathway, which is involved in radiation-induced fibrosis and chronic loss of function after radiation therapy, is affected by HBOT. On the longer term, HBOT reduced the expression of the fibrosis-associated factor α-smooth muscle actin in irradiated salivary glands. This study highlights the potential of HBOT to inhibit the TGFβ-pathway in irradiated salivary glands and to restrain consequential radiation induced tissue injury.
Online address: http://www.molmed.org
doi: 10.2119/molmed.2014.00003

INTRODUCTION

Treatment of head and neck cancer routinely involves radiation therapy (RT), which not only affects tumor tissue, but also the surrounding healthy tissues. Because of their position, salivary glands are often in the radiation portal. Radiation-induced damage to salivary glands is irreversible and results in chronic hyposalivation and a change in saliva composition, leading to a subjective feeling of a dry mouth called xerostomia which greatly affects quality of life. Despite salivary gland sparing techniques such as intensity modulated radiation therapy (IMRT), the surgical transfer of major salivary glands outside the radiation field and the use of cytoprotectants, xerostomia remains a significant problem after radiotherapeutic treatment of malignancies in the head and neck area (1).

Unlike other slowly dividing tissues, salivary glands respond acutely to radiation treatment. Whereas acinar cell number remains unaltered, salivary flow rates drop dramatically at early time points after RT (~0–10 d). It has been proposed that this is due to radiation-induced damage to the plasma membranes, since no cell loss is visible yet (2,3). In the chronic stage of radiation damage (~120–240 d), a lack of functional acinar cells and replacement by connective tissue and fibrosis causes the diminished salivary flow (4). In this phase, some generation of acinar cells does take place, but it is suggested that the new cells cannot function properly due to damage of ducts, blood vessels and nerves (5).

Hyperbaric oxygen therapy (HBOT), in which patients breathe 100% oxygen under elevated pressure, has been used for almost 40 years to treat radiation injuries. Increased oxygen concentration in combination with elevated pressure raises tissue oxygen tension up to ten times. As oxygen under pressure is dissolved in plasma, it can reach otherwise hypoxic areas with obstructed blood flow, like radiation-injured tissues. In the

Address correspondence to *Linda Spiegelberg, Department of Oral & Maxillofacial Surgery, Erasmus MC, Room Ee 15.93, PO Box 2040, 3000 CA Rotterdam, The Netherlands. Phone: +31 (0) 10 7043788; Fax: +31 (0) 10 7044685; E-mail: L.spiegelberg@erasmusmc.nl.*
Submitted January 9, 2014; Accepted for publication May 12, 2014; Epub (www.molmed.org) ahead of print May 13, 2014.

case of the prevention or treatment of xerostomia, some clinical trials report positive effects of HBOT (6–8), mostly measured by quality of life questionnaires. Experimental evidence on the beneficial effects of HBOT on irradiated salivary glands is however scarce (9). In a previous study we showed an increased blood vessel density in irradiated mouse salivary glands in response to HBOT (10). In other tissues and cells, it has been shown that vascular endothelial growth factor (VEGF) levels can rise in response to HBOT (11,12), and angiogenesis can be promoted (13,14). Besides influencing angiogenesis, oxygen also is involved in other key processes associated with wound healing, such as modulating cytokine release, accelerating microbial oxidative killing, modulating leukocyte activation and adhesion, and reducing apoptosis (15). The effects of HBOT on gene expression have been analyzed *in vitro* in neurons, osteoblasts and endothelial cells, maximally 24 h after a single HBO treatment (16–18). In all three cell types, an upregulation of the oxidative stress response was reported. In an *in vivo* model of rat ischemic brain, genes of the neurotrophin system and inflammatory immune response were affected after five consecutive HBO treatments (19). In patients with nonhealing wounds, an upregulation of genes involved in extracellular matrix remodeling and angiogenesis was reported after HBOT (19,20).

Thus far, the effects of HBOT on gene expression in irradiated tissues have not been studied in an *in vivo* model. In this study, we explore the molecular pathways that are influenced by HBOT in irradiated salivary glands of mice by means of microarray analysis. By understanding basic HBOT mechanisms, the clinical implementation of HBOT for accepted indications can be improved.

MATERIALS AND METHODS

Animals

Female C3H mice, 7–9 wks old, were treated with radiotherapy (RT) and/or hyperbaric oxygen therapy (HBOT) as described before (21). The experimental protocol was approved by the Animal Care Committee of Erasmus MC, Rotterdam, the Netherlands (protocol IDs 133-08-09 and 133-11-04), under the national Experiments on Animals Act and adhered to the rules laid down in this national law that serves the implementation of the guidelines on the protection of experimental animals from the Council of Europe (1986), Directive 86/609/EEC (22).

Radiation Therapy (RT)

Radiation therapy was performed as described previously (10). In short, mice were anesthetized intraperitoneally with a mixture of ketamine and xylazine (120 mg/kg and 6 mg/kg body weight, respectively) and irradiated locally in the head and neck area with a single dose of 15 Gy by a 250 kV orthovoltage irradiator (Philips RT250) using a Cu filter and a dose rate of 1.9 Gy/min (Philips Medical Systems, Brussels, Belgium). The rest of the body was shielded by a 0.5-cm lead plate.

Hyperbaric Oxygen Therapy

Hyperbaric oxygen therapy was performed in a custom-built hyperbaric oxygen chamber for small laboratory animals (Hytech BV, Raamsdonksveer, the Netherlands) (23). HBOT was given once a day for five consecutive days a week, with a maximum of 20 sessions. Each session consisted of compression to 2.4 atmospheres absolute (ATA) and 100% oxygen during 30 min, isopression for 60 min, in which pressure and oxygen levels were kept constant and decompression to 1 ATA during 15 min. For animals that were treated with RT, HBOT started the day after.

RNA Isolation

Mice were euthanized by CO_2-asphyxiation and submandibular salivary glands were removed, snap frozen in liquid nitrogen and stored at –80°C until total RNA isolation was performed using the RNeasy Mini Kit (Qiagen, Hilden, Germany) according to the manufacturer's instructions.

Microarray Analysis

Microarray analysis was performed on RNA samples of submandibular glands of untreated mice (control), mice treated with 10 sessions of HBOT (HBOT), mice treated with RT at 2 wks after RT (RT) and mice treated with RT and HBOT at 2 wks after RT (RT + HBOT; n = 4 for each group). Assessment of total RNA quality and purity was performed with the RNA 6000 Nano assay on the Agilent 2100 bioanalyzer (Agilent Technologies, Palo Alto, CA, USA). cDNA was synthesized from total RNA using the IVT Express Labeling kit (Affymetrix, Santa Clara, CA, USA). Subsequent biotin-labeled cRNA synthesis, purification and fragmentation were performed according to the manufacturer's recommendations. A total of 12.5 µg fragmented biotinylated cRNA was subsequently hybridized onto Affymetrix Mouse Genome 430 2.0 Array chips. Image analysis was performed using GeneChip Operating Software with the Affymetrix GeneChip Scanner 3000 according to the manufacturer's protocol. Microarray Suite software (Affymetrix) was used to generate .dat and .cel files. To examine the quality of the various arrays, several R packages (including affyQCreport [24]) were run starting from the .cel files. All created plots, including the percentage of present calls, RNA degradation, NUSE and RLE indicated a high quality of all samples and an overall comparability. Raw intensity values of all samples were normalized by RMA normalization (Robust Multichip Analysis) (background correction and quantile normalization) using Partek version 6.4 (Partek Inc., St. Louis, MO, USA).

The normalized datafile was transposed and imported into OmniViz version 6.0.1 (BioWisdom Ltd., Cambridge, UK) for further analysis. For each probe set, the geometric mean of the hybridization intensity of all samples was calculated. The level of expression of each probe set was determined relative to this

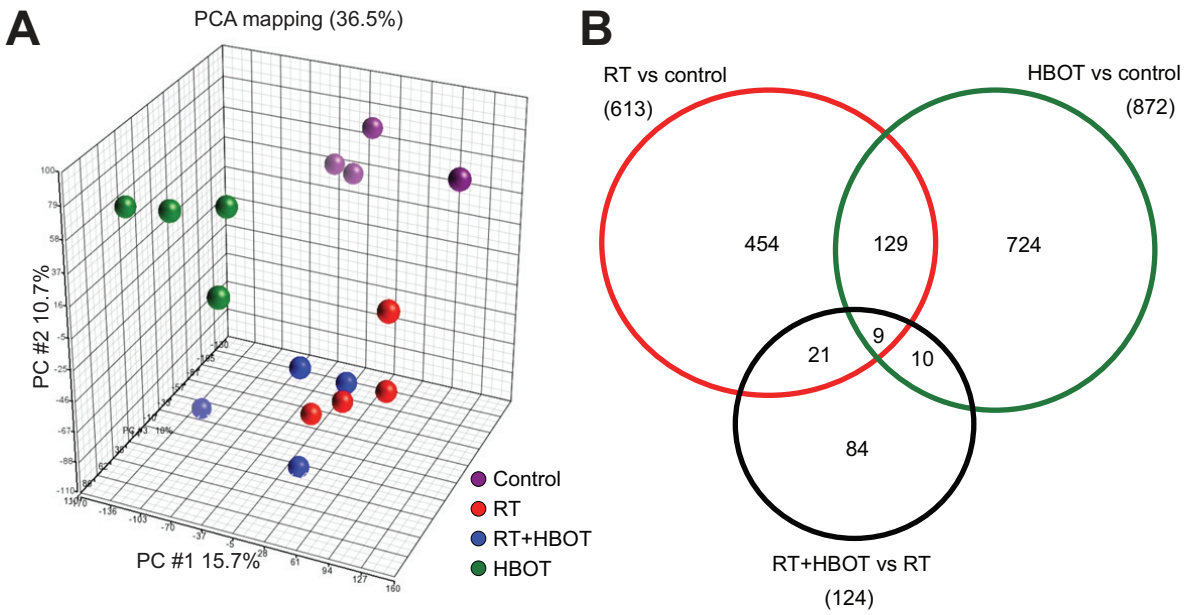

Figure 1. Summary of microarray data by PCA and Venn diagrams. (A) PCA-mapped scatter plot. The global gene expression profiles of the submandibular glands for different treatment groups and control analyzed by PCA. The figure represents the first three principal components of microarray analysis data (PC1, PC2 and PC3) in *x*, *y* and *z* axes, respectively. (B) Venn diagram that represents the number of differentially expressed Affymetrix probe sets in RT versus control (red circle), HBOT versus control (green circle) and RT + HBOT versus RT (black circle), with the number overlapping probe sets inside the circles.

geometric mean and $\log_2$-transformed. The geometric mean of the hybridization signal of all samples was used to ascribe equal weight to gene expression levels with similar relative distances to the geometric mean. Differentially expressed genes were identified using statistical analysis of microarrays (SAM). Cutoff values for significantly expressed genes were a false discovery rate (FDR) of 0.1 or less and a fold change of ≥1.5.

Functional Annotation

Functional annotation of the statistical analysis of microarrays results was done using Ingenuity Pathway Analysis (Ingenuity, Mountain View, CA, USA). The results are shown for biological processes, which are significantly ($P < 0.05$) enriched after multiple testing.

Quantitative Real-Time Reverse Transcription Polymerase Chain Reaction

Total RNA from submandibular glands of four animals per experimental group was reverse transcribed using the iScript cDNA Synthesis Kit (Bio-Rad Laboratories, Hercules, CA, USA). The resulting cDNA was amplified in 40 cycles (enzyme activation at 95°C for 20 s, denaturation at 95°C for 3 s, annealing/extension at 60°C for 30 s) with a Bio-Rad CFX 96 Real-Time Detection System (software version Bio-Rad CFX Manager 2.0) using Fast SYBR Green Master Mix (Applied Biosystems, Life Technologies Europe BV, Bleiswijk, the Netherlands) and primers for: α smooth muscle actin (*α-Sma*), B-cell translocation gene 2 (*Btg2*), Cd83 antigen (*Cd83*), connective tissue growth factor (*Ctgf/Ccn2*), cysteine rich protein 61 (*Cyr61/Ccn1*), early growth response 1 and 2 (*Egr1* and *Egr2*), glyceraldehyde-3-phosphate dehydrogenase (*Gapdh*), serpin peptidase inhibitor, calde E, member 1 (*Serpine1/Pai1*), SRY-box containing gene 2 (*Sox2*), transferring receptor (*Tfrc*), transforming growth factor β 1 (*Tgfβ1*) and thrombospondin 1 (*Thbs1*). For primer sequences see Supplementary Table S1). Each PCR reaction was performed in duplicate and the average threshold cycle (Ct) value was used for relative quantification of gene expression compared with the housekeeping gene Gapdh, with the comparative Ct method ($\Delta\Delta C_T$).

(Immuno-)Histochemistry

Immediately after euthanization, submandibular glands were excised and stored in 10% buffered formalin for 24 to 36 h. Tissues were then dehydrated, embedded in paraffin blocks and 5-µm slides were cut. Standard hematoxylin and eosin (H&E) and picrosirius red stainings were performed to visualize fibrosis and collagen content. For the detection of TGFβ1, Serpine1 and α-SMA, sections blocked with 5% nonfat milk powder and then probed with a primary antibody against TGFβ1 (1:50, Santa Cruz Biotechnology Inc, Dallas, USA), Serpine1 or α-SMA (1:100, Novus Biologicals Ltd., Cambridge, UK) overnight at 4°C. Biotinylated goat anti-rabbit IgG (Dako, Carpinteria, CA, USA) was used as secondary antibody (30 min at room temperature). Detection of the antibody complex was performed with streptavidin–peroxidase

Table 1. Cellular and physiological functions.[a]

	Category	Functional Annotation	*p* Value	Activation *z* score
RT	Cell death and survival	apoptosis	4.14E-12	–1.285
		necrosis	8.00E-12	–0.863
		cell death	4.68E-10	–1.104
		cell death of connective tissue cells	6.76E-10	0.515
		cell survival	9.86E-08	2.742
	Cell cycle	arrest in interphase	5.19E-11	
		interphase	2.26E-10	0.512
		cell cycle progression	6.63E-09	2.092
		G1 phase	3.74E-07	–0.018
	Gene expression	binding of DNA	4.58E-10	–0.274
		transcription of RNA	1.01E-07	0.441
		binding of protein binding site	3.47E-07	0.839
		expression of RNA	5.59E-07	0.914
		expression of DNA	5.96E-06	1.485
	Cellular growth, development and proliferation	proliferation of cells	7.07E-09	0.710
		proliferation of connective tissue cells	4.59E-08	1.905
		differentiation of connective tissue cells	6.38E-08	2.668
		differentiation of cells	2.20E-07	1.256
HBOT	Cellular function and maintenance	function of leukocytes	2.57E-14	–0.751
		function of blood cells	3.58E-13	–0.751
		function of mononuclear leukocytes	1.20E-09	–0.684
		function of lymphocytes	3.20E-09	–0.684
	Cellular movement	chemotaxis of leukocytes	1.46E-11	–3.641
		cell movement of leukocytes	1.68E-11	–4.942
		homing of leukocytes	4.30E-11	–3.753
		chemotaxis of myeloid cells	6.64E-11	–3.110
	Cellular development	proliferation of lymphocytes	2.00E-10	–2.036
		proliferation of immune cells	7.99E-10	–2.268
		proliferation of blood cells	1.45E-09	–2.083
	Cell-to-cell signaling and interaction	activation of cells	2.32E-10	–3.952
		activation of leukocytes	3.17E-10	–4.119
		activation of blood cells	2.04E-09	–3.932
RT + HBOT	Cellular growth, development and proliferation	proliferation of cells	6.44E-08	2.676
		proliferation of fibroblast cell lines	4.57E-05	0.873
		differentiation of connective tissue cells	1.52E-04	2.074
		formation of cells	1.95E-04	0.528
		proliferation of connective tissue cells	4.71E-04	1.728
	Cell death and survival	necrosis	3.13E-06	–0.182
		cell death	7.26E-06	–0.101
		apoptosis	8.46E-06	–0.521
		cell viability of fibroblasts	3.66E-04	0.647
	Cell cycle	arrest in G1 phase	6.09E-05	
		polyploidization of cells	1.30E-04	–0.640
		arrest in interphase	1.77E-04	
	Cellular function and maintenance	transport of D-glucose	3.38E-05	2.419
		concentration of D-glucose	8.41E-05	–0.491
		quantity of carbohydrate	2.69E-04	0.585

[a]Cellular and physiological functions that are affected by RT, HBOT and RT + HBOT, divided into categories. *z* Scores of <2 (inhibition) or >2 (activation) are considered statistically significant.

(R&D Systems, Oxon, UK) and 3,3′-diaminobenzidine (Dako). Hematoxylin served as counterstain.

Quantification

Slides stained for α-SMA were scanned using a slide scanner (Hamamatsu Photonics KK, Japan). A representative 10× magnified picture was taken for each gland and α-SMA staining was analyzed by Cell[d] (Olympus Life Science Europe GmbH) to detect the percentage of α-SMA positive staining.

Statistical Analysis

All data are expressed as mean values with standard deviation (SD), and were analyzed using SPSS PASW 17.0 for Windows (SPSS Inc., Chicago, IL, USA). Univariate tests with *post hoc* Bonferroni correction were used to identify statistical differences ($P < 0.05$) between groups.

All supplementary materials are available online at www.*molmed.org*.

RESULTS

Gene Expression Analysis of Submandibular Glands

To investigate the effect of hyperbaric oxygen therapy on molecular pathways in irradiated and nonirradiated salivary glands, gene expression analysis was performed on submandibular salivary glands of control mice, irradiated mice two weeks after radiotherapy (RT), mice treated with daily hyperbaric oxygen therapy for two weeks (HBOT) and irradiated mice treated with hyperbaric oxygen therapy for two weeks (RT + HBOT) (n = 4/group). Principal component analysis (PCA) indicates a clear clustering of groups, with samples of both irradiated groups closest to each other (Figure 1A).

Differentially expressed probe sets were identified in salivary glands of all experimental groups using statistical analysis of microarrays (SAM, ≥ 1.5-fold change, FDR 0.1). Treatment with RT or HBOT resulted in a change in expression levels of 613 probe sets and 872 probe sets, respectively. Treatment of irradiated glands with HBOT led to the identification of 124 differentially expressed probe sets, of which 84 were unique to this group (Figure 1B), indicating that HBOT has a different effect on irradiated and healthy glands. The lists of significantly up- and downregulated genes of the different groups are shown in Supplementary Tables S2–S5. These sets of up- and downregulated genes were used for further functional annotation of pathways and functional categorization using Ingenuity Pathway Analysis (IPA). The canonical pathways that were affected by RT were anticipated for on the basis of existing knowledge and included the P53 and ATM signaling, NRF2-mediated oxidative response and the acute phase response. Table 1 shows cellular and physiological functions that are most significantly influenced by RT, HBOT or RT + HBOT. Irradiated salivary glands of the groups with and without HBOT showed clear differential expression of genes that enhance survival, cell proliferation and differentiation of connective tissue cells. Strikingly, apoptosis was re-

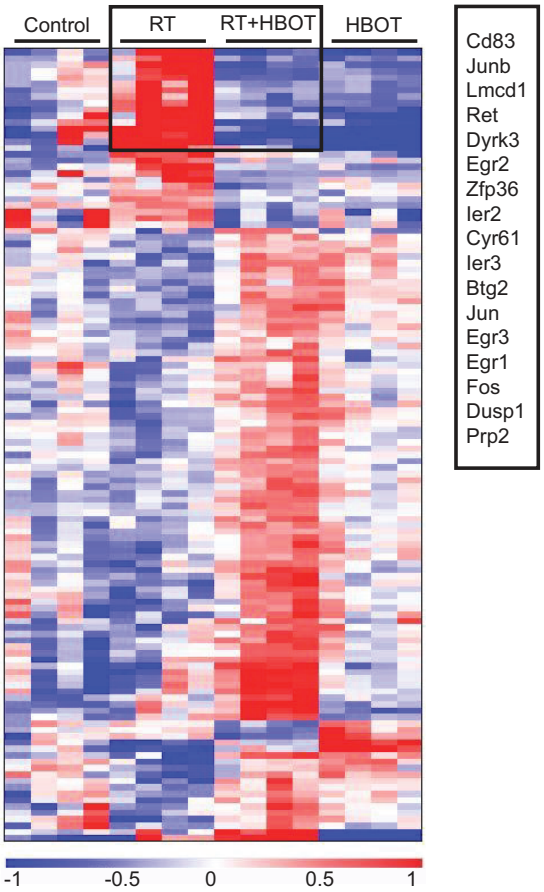

Figure 2. Differentially expressed probe sets between the RT– and RT + HBOT group. OmniViz treescape showing the hierarchical clustering of differentially expressed Affymetrix probe sets between the submandibular glands of the RT and RT + HBOT group (middle groups). Expression of these probe sets for the control and HBOT-group is shown on the outside. Red indicates upregulated probe sets compared with the geometric mean and blue indicates downregulated probe sets compared with the geometric mean. The color intensity correlates with the degree of change. Rectangle shows probe sets that are upregulated in the RT group, while downregulated in the RT + HBOT group. Genes within this rectangle are summarized.

Table 2. Upstream regulators.[a]

	RT versus control		RT + HBOT versus RT	
Upstream regulator	Activation *z* score	*p* Value	Activation *z* score	*p* Value
PDGF BB	5.039	6.79E-23	–3.449	1.91E-09
EGF	4.835	6.21E-20	–3.378	6.88E-12
TGFB1	3.632	4.02E-14	–3.175	1.60E-05
IL1B	2.506	5.82E-22	–2.829	2.42E-05
IL4	3.040	1.18E-06	–2.771	9.84E-04
TNFSF11	3.330	5.31E-05	–2.741	1.54E-05
P38 MAPK	3.598	2.71E-14	–2.731	3.68E-07
IL3	3.450	2.44E-07	–2.728	2.08E-05
FGF2	4.145	6.45E-10	–2.601	5.14E-04
CSF2	3.475	2.42E-07	–2.587	1.32E-04
Pkc(s)	3.703	1.73E-08	–2.503	6.37E-06
F2	4.361	1.01E-10	–2.442	1.60E-06
Ins1	3.030	2.57E-06	–2.439	1.04E-05
MAPK14	2.345	1.80E-06	–2.433	9.74E-07
CHRM1	2.423	1.09E-07	–2.423	6.17E-12
Jnk	3.647	8.55E-09	–2.414	4.30E-06
CSF3	3.109	2.81E-03	–2.401	6.07E-06
NfkB (complex)	3.823	4.77E-14	–2.396	3.32E-06
CSF1	2.964	4.82E-06	–2.375	8.40E-05
LEP	2.225	7.91E-08	–2.371	2.65E-03
ERK	3.772	1.41E-10	–2.258	2.58E-07
CREBBP	2.411	2.07E-09	–2.219	6.03E-07
EPHB1	2.425	5.06E-08	–2.216	7.11E-10
GNRH1	2.763	1.84E-05	–2.202	1.27E-06
IGF1	3.595	5.00E-19	–2.197	2.51E-06
Gm-csf	2.391	5.55E-04	–2.189	1.87E-06
POMC	2.404	1.36E-02	–2.187	3.77E-05
F7	2.934	2.63E-08	–2.183	3.11E-07
Il1A	2.391	4.43E-04	–2.168	1.63E-03
ELK1	2.542	7.79E-07	–2.146	9.07E-09
AGT	2.953	5.97E-07	–2.047	2.15E-05

[a]Upstream regulators that were predicted to be activated by RT, and inhibited when HBOT was applied after RT, on the basis of the microarray data of the submandibular glands. *z* Scores of <2 (inhibition) or >2 (activation) are considered significant.

Table 3. Genes of interest.[a]

Process	Gene	RT versus control (fold change)	RT + HBOT versus RT (fold change)
Fibrosis	*Cyr1*	+4.3	–4.6
	Ctgf	+3.4	
	Egr1	+6.5	–12.2
Regeneration	*Btg2*	+2.9	–4.9
	Sox2		+2.6
	Tfrc		+2.6
Immune response	*Cd83*	+2.3	–2.2

[a]Genes of interest that were selected for qPCR validation with fold changes from the microarray.

duced and cell survival enhanced. HBOT resulted in a change in a remarkable number of functions associated with the immune response and inflammation in the salivary glands of nonirradiated mice. No such strong immunological response of HBOT was detected in the irradiated tissue. To elaborate on the influence of HBOT on irradiated tissues, the expression levels of the differentially expressed genes of the RT + HBOT versus the RT group were analyzed by treescape and revealed a group of genes that was upregulated after RT, but significantly downregulated if HBOT was applied after RT (Figure 2). This group consisted mostly of immediate early response genes like *Fos*, *Jun* and members of the *Egr* and *Ier* family, indicating that HBOT can prevent or inhibit the radiation-induced expression of these genes.

By using the Ingenuity software, activation or inhibition of upstream regulators was predicted on the basis of up- and downregulated genes in the dataset. In this way, regulatory cascades and biological activities occurring in the tissue were determined. Table 2 shows the list of RT-activated regulators that were significantly inhibited after HBOT treatment, a considerable amount of which are cytokines and growth factors known to play roles in radiation-induced processes such as fibrosis, apoptosis, tissue regeneration and inflammation.

qPCR Validation

On the basis of their expression profiles and putative roles in tissue repair, nine genes of interest were selected for qPCR-validation (Table 3). The first group consisted of genes that are linked to fibrosis and that were significantly downregulated by HBOT in irradiated salivary glands while upregulated by RT alone: *Egr1*, *Egr2* and *Cyr61*. *Ctgf* was included because of its direct link to fibrosis and the fact that it was less upregulated in irradiated glands after HBOT treatment as well.

On the basis of their differential expression patterns, *Btg2* (antiproliferative

capacities), *Sox2* (stem cell maintenance), *Tfrc* (control of cell proliferation and growth) and *Thbs1* (negative regulation of regeneration and angiogenesis) were selected because of their putative roles in regeneration. In addition, *Cd83* was included in the qPCR analysis as it is involved in the immune response and was affected considerably by HBOT according to the microarray analysis. By qPCR, differential expression was confirmed for all selected genes, although for *Egr2* and *Thbs1*, the differences were not statistically significant (Figure 3).

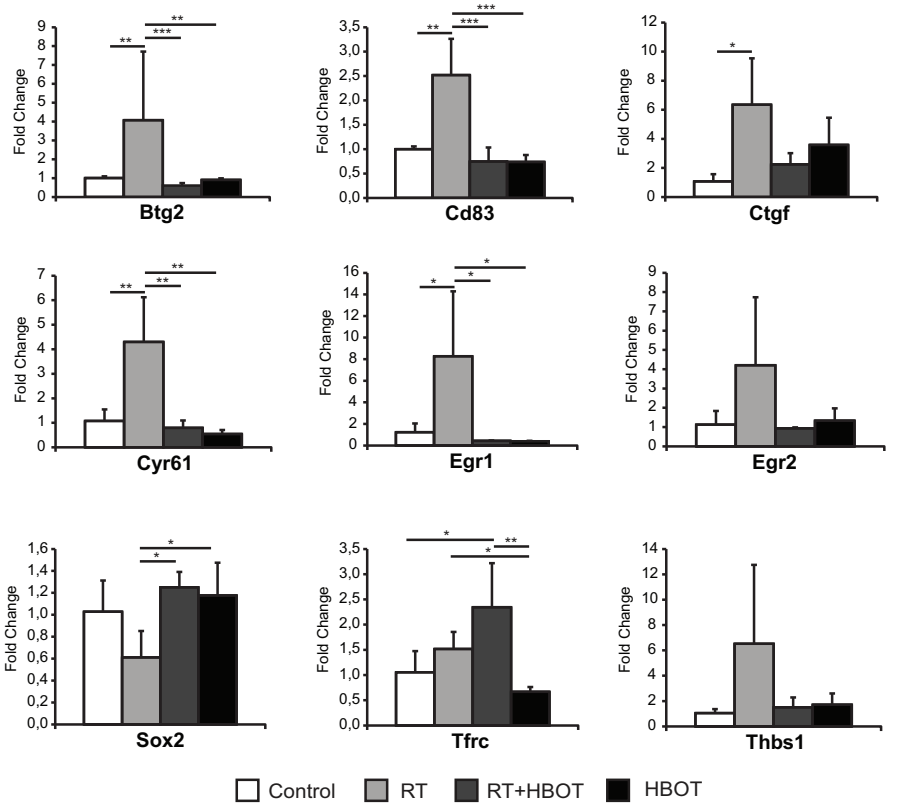

Figure 3. qPCR validation of genes of interest. qPCR validation of microarray results for the expression of genes of interest at 2 wks after RT in the submandibular glands. *y* Axis shows mean fold change relative to controls. Lines above bars represent statistically significant differences (*$P < 0.05$, **$P < 0.01$, ***$P < 0.001$).

TGFβ-Pathway

Because of its known role in (radiation-induced) fibrosis, we further analyzed the TGFβ-pathway in our dataset using IPA. The TGFβ1 regulator pathway was predicted to be activated in the RT group and to be inhibited if HBOT was applied after RT (see Table 2). Figure 4 shows an upregulation of a set of target genes of the canonical TGFβ1-pathway in the RT group compared with controls (Figure 4A), and an inhibition when HBOT was given to irradiated tissue (Figure 4B). Expression analysis of the *Tgfβ1* gene and its effector gene *Serpine1* by qPCR at 2 wks after RT was performed to confirm the inhibitory effect of HBOT on the TGFβ-pathway (Figure 4C). Both genes showed lower expression 2 wks after RT if HBOT had been applied. Immunohistochemical staining for TGFβ1 and Serpine1 also showed an RT-induced upregulation that was partly counteracted by HBOT (Figure 4D). The expression of *α-SMA*, which is a profibrotic factor expressed by myofibroblasts, but also by myoepithelial cells in the salivary gland, showed a similar pattern with higher expression in the RT-treated group at 2 and 10 wks after RT (Figure 5A). Immunohistochemistry showed a significantly higher expression in RT-treated glands at 24 wks after RT compared with irradiated glands that received HBOT (Figure 5B). Although expression analysis showed a potential inhibitory effect of HBOT on profibrotic markers, we were unable to identify major signs of fibrosis in H&E- and picrosirius red–stained tissue, at 2, 10 and 24 wks after RT.

DISCUSSION

Radiation-induced damage to salivary glands is a serious, irreversible complication of RT to the head and neck region. Hyperbaric oxygen therapy is used in the treatment of radiation-induced injury to normal tissues in the head and neck region while its mechanism of action remains poorly understood. Especially, little is known about the molecular pathways that are influenced by HBOT on irradiated salivary glands. Therefore, we investigated the effects of radiotherapy and HBOT on gene expression in submandibular glands of mice, 2 wks after a single dose of 15 Gy and after 10 consecutive HBO treatments.

As expected, RT resulted in the activation of pathways involved in cell cycle and DNA damage repair, such as the p53 pathway, the NRF2-mediated oxidative response and the acute phase response signaling. HBOT did not have an effect on these pathways. The microarray data predict that RT has an inhibiting effect on apoptosis and increases cell survival 2 wks after irradiation. This apoptotic response may seem unexpected since it is known that p53 signaling after irradiation leads to apoptosis (25) and apoptosis of acinar cells after RT of salivary glands has been reported (26). However, in response to RT, pro- as well as antiapoptotic and cell survival signaling pathways are activated, which occurs in waves. For instance, to allow DNA repair to take place after RT-induced damage, specific signaling pathways stimulate cell

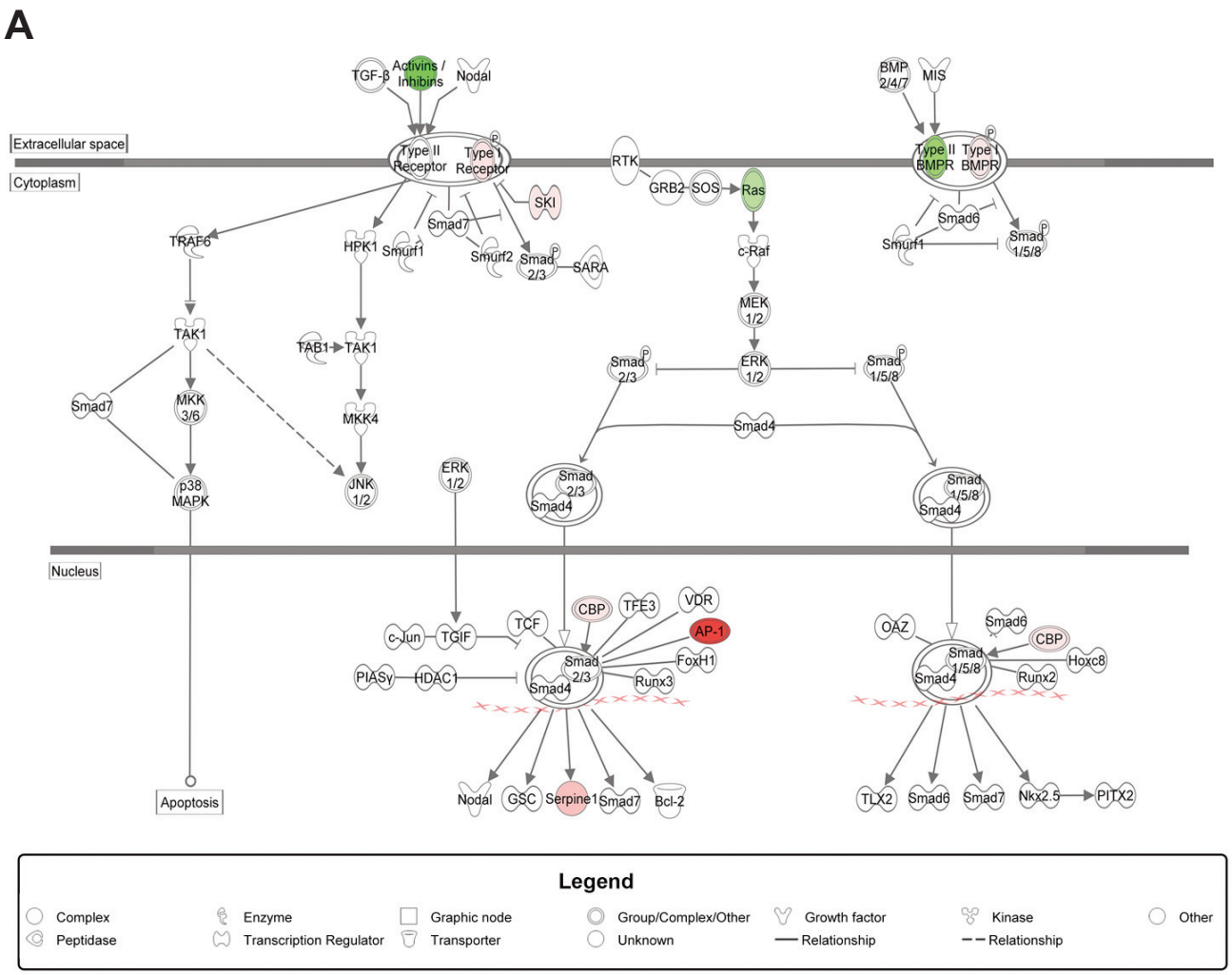

Figure 4. Influence of HBOT on the TGFβ-pathway. Differential expression of genes involved in the TGFβ-pathway in irradiated submandibular glands compared with control (A) and in irradiated glands that received HBOT compared with irradiated glands (B), by Ingenuity Pathway Analysis of microarray data. Colors show up- (red) and downregulated (green) genes (≥ 1.2-fold change, FDR 0.05). Notice the reverse expression of genes when HBOT is applied to irradiated glands. qPCR validation (C) and immunohistochemical staining (D) of Tgfβ1 and Serpine1 at 2 wks after RT. Scale bars left pictures 200 μm, right pictures 50 μm.

Continued on next page

cycle arrest and prevent apoptosis (27,28). The balance between these pathways will decide whether more pro- or antiapoptotic proteins will be expressed (28). Our microarray data don't reveal significant effects of HBOT on apoptosis or cell survival pathways, which corresponds to our previous histological study in which no profound effect of HBOT on apoptosis levels was detected in salivary glands after RT (10).

Radiation causes vascular damage and thereby hypoxia (29). It is generally assumed that HBOT can positively influence angiogenesis (reviewed in [30]). In a previous study, we showed an increased blood vessel density due to HBOT in irradiated submandibular glands of mice at ten weeks after RT (10). The microarray performed in the present study, at 2 wks after RT, did not show a discernible effect of HBOT on gene expression profiles associated with angiogenesis, possibly because the 2-wk time point is too early to detect these effects.

In healthy submandibular glands, HBOT led to a remarkable amount of differentially expressed probe sets, even more than RT alone (872 versus 613 probe sets) indicating that HBOT induces changes in healthy, nonhypoxic tissue. In particular biological functions that are associated with the immune system, such as the movement, activation and adhesion of different immunological cells, were decreased by HBOT. In a wound model, suppressive effects of HBOT on the expression of inflammatory

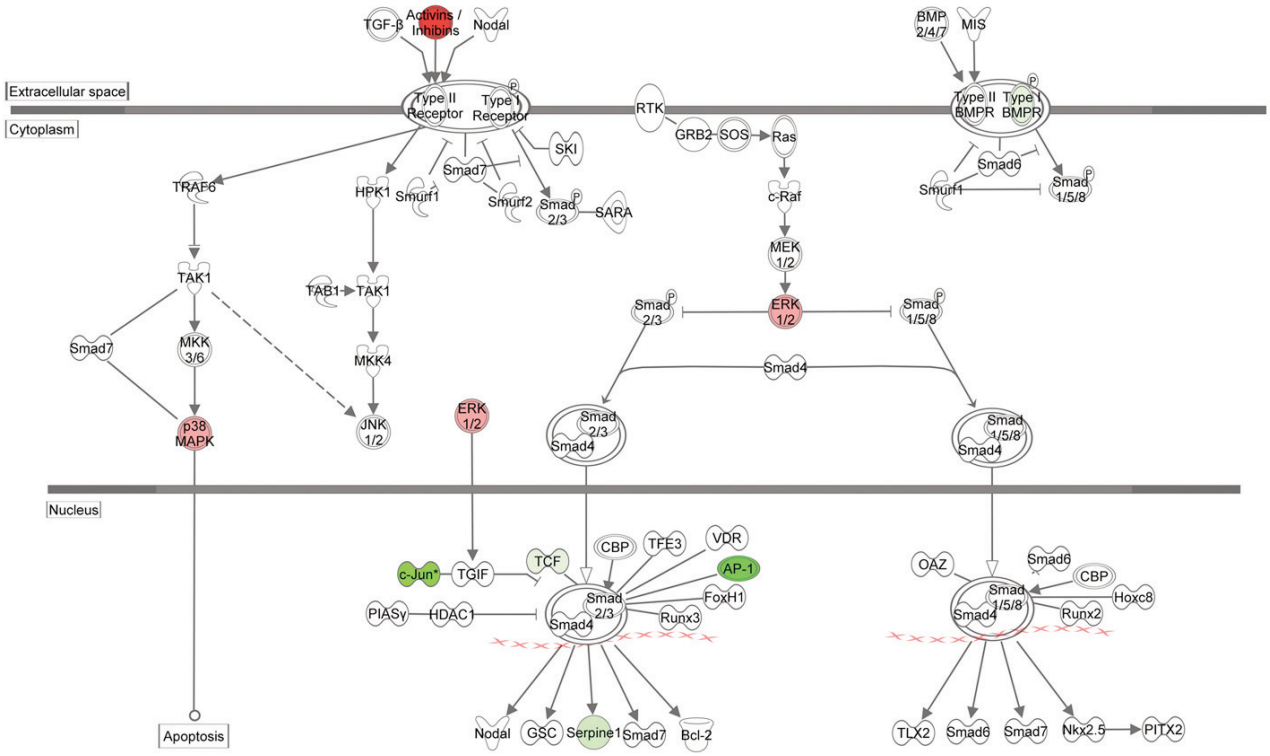

Figure 4. ***Continued.***

Continued on next page

genes have been described and are a basis of its use in treating chronic (diabetic) wounds (31–33).

Genes that were most upregulated by RT included the early response genes *Fos*, *Jun* and *Egr1*. This upregulation has been reported before in mammalian cells shortly after RT (34,35) and our *in vivo* model shows that this upregulation still persists 2 wks after RT. Interestingly, HBOT significantly downregulated the expression of these early response genes, when applied in irradiated salivary glands, indicating a counteraction of HBOT on RT-induced mechanisms. Strikingly, the predicted activation of the TGFβ1 regulatory pathway by RT appears to be significantly attenuated if HBOT is applied. The TGFβ-pathway is strongly associated with radiation-induced fibrosis in different organs, and is the subject of investigation regarding possible antifibrotic therapies (36–39).

This pathway regulates the formation of extracellular matrix (ECM), and has been shown to be activated by RT (40–43). The binding of TGFβ to its receptor can lead, via Smad dependent and independent pathways, to the expression of target genes such as *Ctgf* and *Serpine1*. CTGF stimulates differentiation of fibroblasts to myofibroblasts, which express α-SMA and produce (components of the) ECM. Serpine1 is a protease inhibitor which suppresses matrix metalloproteases (MMPs) from breaking down ECM and is thus matrix preserving (44,45). Excessive matrix formation/preservation leads to fibrosis since functional cells are replaced by ECM leading to dysfunction of the tissue (38). Conditional overexpression of *Tgfβ1* has been shown to induce fibrosis in salivary glands of mice as seen under pathological conditions (46).

Different genes that were upregulated by RT and downregulated when HBOT was applied to irradiated tissue are involved in the TGFβ-pathway. Increased *Egr1* and *Egr2* expression have been postulated as key mediators of TGFβ signaling and fibrosis and thereby as potential targets for antifibrotic therapy (47–50). *Cyr61*, which is a member of the CTGF family, can be regulated by *TGFβ* and has proinflammatory properties (51,52). THBS1 is an activator of latent TGFβ so it can bind to its receptor (53). All together, our microarray results indicate that the TGFβ-pathway is repressed by HBOT in irradiated tissue, which was confirmed by immunohistochemical staining for TGFβ1 and Serpine1. Staining for α-SMA in the submandibular glands also showed an HBOT-induced decrease at 24 wks after RT. Myofibroblasts express α-SMA, but it is also expressed by myoepithelial cells that are abundant in the salivary glands. Myoepithelial cells can differentiate into myofibroblasts by epithelial-to-

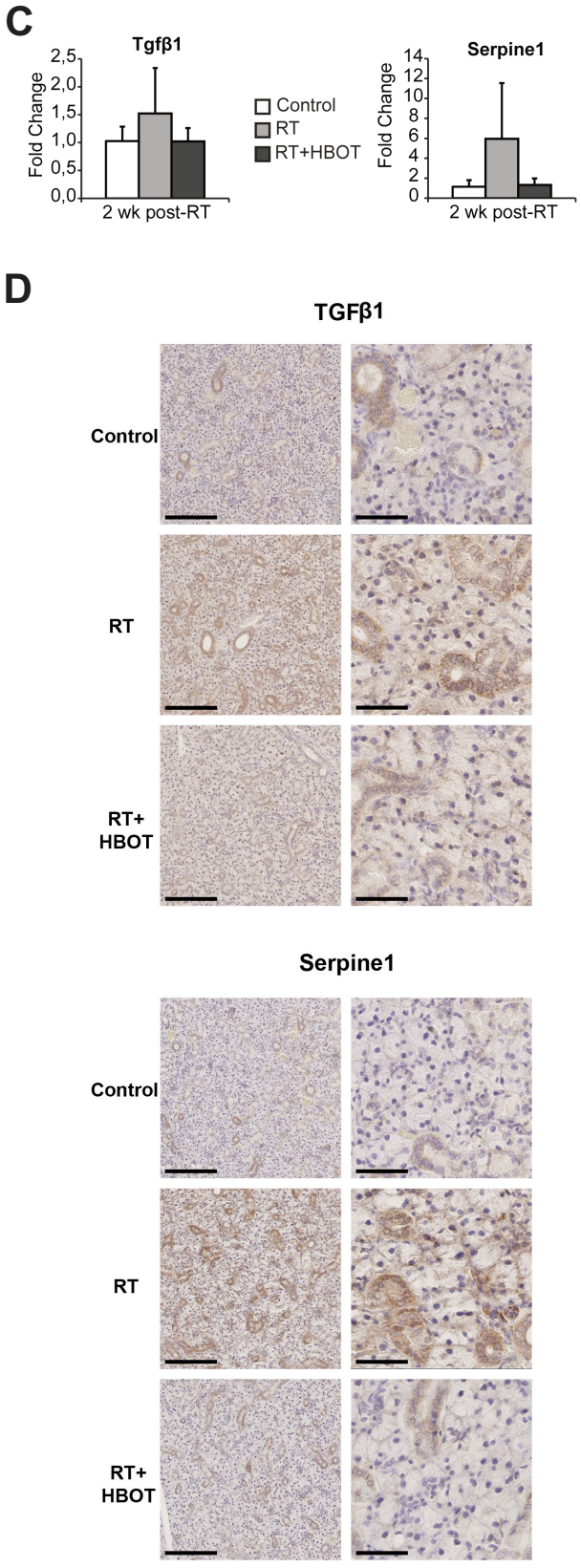

Figure 4. *Continued.*

mesenchymal transition (EMT), a process that is induced by TGFβ and is known to contribute to fibrosis (54,55). Fibrosis or higher collagen content was not detected in the submandibular glands at any of the time points studied, but the higher expression level of α-SMA in the RT- group could precede fibrosis. Presumably in our model, fibrosis is not yet revealed at 24 wks after RT. It has been shown that irradiation-induced lung fibrosis in mice can take 30 wks to develop and is highly strain-dependent (56).

An effect of HBOT on TGFβ signaling *in vivo* has been observed before in non-irradiated tumor tissue by Moen *et al*. (57). They found reduced *Tgfβ* expression after HBOT and stated that HBOT is able to induce mesenchymal-to-epithelial transition (MET), the opposite of EMT. *In vitro*, TGFβ expression and secretion by fibroblasts has been shown to be decreased in response to HBOT (12,58). A reduction of fibrosis by HBOT has been demonstrated in animal models of laminectomy, tracheal anastomosis and myocardial infarction (59–61), although in a tendon healing model, HBOT seemed to enhance fibrosis (62).

Except for TGFβ1, HBOT was predicted to inhibit other regulatory factors, such as platelet derived growth factor (PDGF). PDGF has been shown to influence the TGFβ-pathway and is implicated to be involved in fibrosis as well (63). The suppression of TGFβ and PDGF as potential antifibrotic therapies is of interest and has been investigated in several studies (37,41). Fibrosis is a complex process involving several pathways that are interconnected and the concurrent suppression of more of these factors is more likely to have an effect on a biological process. Therefore, multitargeted therapies may be more effective and HBOT could potentially be such a therapy.

We cannot distinguish whether 100% oxygen only or 100% oxygen delivery under pressure leads to the reported changes in gene expression. However, HBOT is an established therapy in the treatment of radiation-induced injury

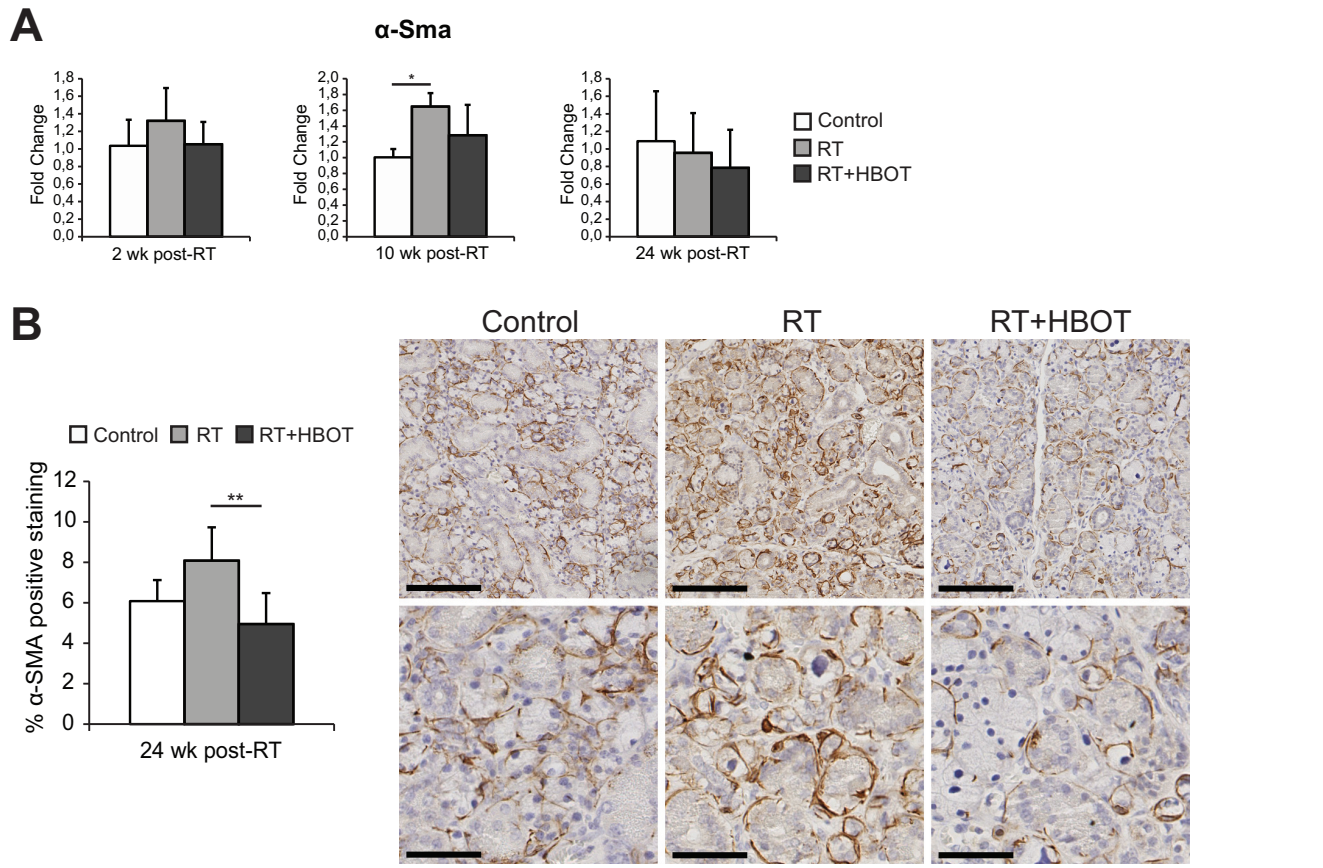

Figure 5. Expression of α smooth muscle actin. Relative expression (mean fold change relative to controls) of α smooth muscle actin (α-Sma) at 2, 10 and 24 wks after RT in the submandibular glands (A). Line above bars represents statistically significant difference (*$P < 0.05$). Immunohistochemical staining of α-SMA in submandibular glands of control and irradiated mice, either with hyperbaric oxygen therapy (RT + HBOT) or without (RT). Graph shows the percentage of positive α-SMA staining for the different groups (B). Line above bars represents statistically significant difference (**$P < 0.01$; $P = 0.053$ for RT versus control). Scale bars upper pictures 200 μm, lower pictures 50 μm.

and the elevated pressure has been shown to increase oxygen tension in tissue more than elevated oxygen levels only (64). Under pressure, oxygen concentrations are increased in the plasma, allowing better oxygenation of obstructed tissue areas, since these are not reached by the oxygen that is bound to the hemoglobin of the red blood cells (30). Therefore it is thought that HBOT is more effective in oxygenation and restoration of hypoxic tissues.

CONCLUSION

We showed that HBOT influences a number of pathways and genes in irradiated salivary glands. With respect to radiation-induced damage, the TGFβ-pathway is of particular interest, since it is directly related to the pathogenesis of fibrosis. On the basis of our microarray data, HBOT seems to inhibit the radiation-induced activation of this pathway. In our model, at 24 wks after RT, lower levels of the profibrotic marker α-SMA were detected in the salivary glands of mice that underwent HBOT, indicating that this therapy could possibly affect the process of fibrosis. Therefore it is of interest to further investigate the influence of HBOT on the TGFβ-pathway and fibrosis, not only for salivary glands, but also for other tissues that are sensitive to radiation-induced fibrosis such as lung, kidney, heart and intestine

ACKNOWLEDGMENTS

This research was financially supported by Fonds NutsOhra (grant number 0801-77). We would like to thank Luuk te Riet for his help on the qPCR, Peter van der Spek for the use of Ingenuity and Roland Kanaar for discussing the data.

DISCLOSURES

The authors declare that they have no competing interests as defined by Molecular Medicine, or other interests that might be perceived to influence the re-

sults and discussion reported in this paper.

REFERENCES

1. Radvansky LJ, Pace MB, Siddiqui A. (2013) Prevention and management of radiation-induced dermatitis, mucositis, and xerostomia. *Am. J. Health Syst. Pharm*. 70:1025–32.
2. Konings AW, Coppes RP, Vissink A. (2005) On the mechanism of salivary gland radiosensitivity. *Int. J. Radiat. Oncol. Biol. Phys*. 62:1187–94.
3. Takagi K, *et al*. (2003) Secretion of saliva in X-irradiated rat submandibular glands. *Radiat. Res*. 159:351–60.
4. Grundmann O, Mitchell GC, Limesand KH. (2009) Sensitivity of salivary glands to radiation: from animal models to therapies. *J. Dent. Res*. 88:894–903.
5. Coppes RP, Zeilstra LJ, Kampinga HH, Konings AW. (2001) Early to late sparing of radiation damage to the parotid gland by adrenergic and muscarinic receptor agonists. *Br. J. Cancer* 85:1055–63.
6. Cankar K, Finderle Z, Jan J. (2011) The effect of hyperbaric oxygenation on postradiation xerostomia and saliva in patients with head and neck tumours. *Caries Res*. 45:136–41.
7. Forner L, *et al*. (2011) Does hyperbaric oxygen treatment have the potential to increase salivary flow rate and reduce xerostomia in previously irradiated head and neck cancer patients? A pilot study. *Oral Oncol*. 47:546–51.
8. Teguh DN, *et al*. (2009) Early hyperbaric oxygen therapy for reducing radiotherapy side effects: early results of a randomized trial in oropharyngeal and nasopharyngeal cancer. *Int. J. Radiat. Oncol. Biol. Phys*. 75:711–6.
9. Spiegelberg L, Djasim UM, van Neck HW, Wolvius EB, van der Wal KG. (2010) Hyperbaric oxygen therapy in the management of radiation-induced injury in the head and neck region: a review of the literature. *J. Oral Maxillofac. Surg*. 68:1732–9.
10. Spiegelberg L, *et al*. (2014) Effects of hyperbaric oxygen therapy on the viability of irradiated soft head and neck tissues in mice. *Oral Dis*. 20:e111–9.
11. Sheikh AY, *et al*. (2000) Effect of hyperoxia on vascular endothelial growth factor levels in a wound model. *Arch. Surg*. 135:1293–7.
12. Kang TS, Gorti GK, Quan SY, Ho M, Koch RJ. (2004) Effect of hyperbaric oxygen on the growth factor profile of fibroblasts. *Arch. Facial Plast. Surg*. 6:31–5.
13. Hopf HW, *et al*. (2005) Hyperoxia and angiogenesis. *Wound Repair Regen*. 13:558–64.
14. Tompach PC, Lew D, Stoll JL. (1997) Cell response to hyperbaric oxygen treatment. *Int. J. Oral Maxillofac. Surg*. 26:82–6.
15. Zhang Q, Gould LJ. (2013) Hyperbaric oxygen reduces matrix metalloproteinases in ischemic wounds through a redox-dependent mechanism. *J. Invest. Dermatol*. 134:237–46.
16. Chen Y, Nadi NS, Chavko M, Auker CR, McCarron RM. (2009) Microarray analysis of gene expression in rat cortical neurons exposed to hyperbaric air and oxygen. *Neurochem. Res*. 34:1047–56.
17. Godman CA, *et al*. (2010) Hyperbaric oxygen induces a cytoprotective and angiogenic response in human microvascular endothelial cells. *Cell Stress Chaperones*. 15:431–42.
18. Wong AK, Schonmeyr BH, Soares MA, Li S, Mehrara BJ. (2008) Hyperbaric oxygen inhibits growth but not differentiation of normal and irradiated osteoblasts. *J. Craniofac. Surg*. 19:757–65.
19. Hirata T, *et al*. (2007) The temporal profile of genomic responses and protein synthesis in ischemic tolerance of the rat brain induced by repeated hyperbaric oxygen. *Brain Res*. 1130:214–22.
20. Alleva R, *et al*. (2008) alpha-Lipoic acid modulates extracellular matrix and angiogenesis gene expression in non-healing wounds treated with hyperbaric oxygen therapy. *Mol. Med*. 14:175–83.
21. Spiegelberg L, *et al*. (2013) Effects of hyperbaric oxygen therapy on the viability of irradiated soft head and neck tissues in mice. *Oral Dis*. 20:e111–9.
22. Council of the European Communities. (1986 Dec 12) Council Directive 86/609/EEC of 24 November 1986 on the approximation of laws, regulations and administrative provisions of the Member States regarding the protection of animals used for experimental and other scientific purposes. *Off. J. Eur. Communities*. [cited 2014 Jun 2]; L 358:1–28. Available from: http://eur-lex.europa.eu/legal-content/EN/TXT/?uri=CELEX:31986L0609
23. Djasim UM, Spiegelberg L, Wolvius EB, van der Wal KG. (2011) A hyperbaric oxygen chamber for animal experimental purposes. *Int. J. Oral Maxillofac. Surg*. 41:271–4.
24. Parman C, Halling C and Gentleman R. affyQCReport: QC Report Generation for affyBatch objects. R package version 1.42.0. Available from: http://www.bioconductor.org/packages/2.14/bioc/html/affyQCReport.html
25. Eriksson D, Stigbrand T. (2010) Radiation-induced cell death mechanisms. *Tumour Biol*. 31:363–72.
26. Limesand KH, Said S, Anderson SM. (2009) Suppression of radiation-induced salivary gland dysfunction by IGF-1. *PLoS One*. 4:e4663.
27. Magne N, *et al*. (2006) NF-kappaB modulation and ionizing radiation: mechanisms and future directions for cancer treatment. *Cancer Letters*. 231:158–68.
28. Valerie K, *et al*. (2007) Radiation-induced cell signaling: inside-out and outside-in. *Mol. Cancer Ther*. 6:789–801.
29. Stone HB, Coleman CN, Anscher MS, McBride WH. (2003) Effects of radiation on normal tissue: consequences and mechanisms. *Lancet Oncol*. 4:529–36.
30. Gill AL, Bell CN. (2004) Hyperbaric oxygen: its uses, mechanisms of action and outcomes. *QJM*. 97:385–95.
31. Al-Waili NS, Butler GJ. (2006) Effects of hyperbaric oxygen on inflammatory response to wound and trauma: possible mechanism of action. *ScientificWorldJournal*. 6:425–41.
32. Kendall AC, *et al*. (2012) Changes in inflammatory gene expression induced by hyperbaric oxygen treatment in human endothelial cells under chronic wound conditions. *Exp. Cell Res*. 318:207–16.
33. Zhang Q, Chang Q, Cox RA, Gong X, Gould LJ. (2008) Hyperbaric oxygen attenuates apoptosis and decreases inflammation in an ischemic wound model. *J. Invest. Dermatol*. 128:2102–12.
34. Weichselbaum RR, Hallahan D, Fuks Z, Kufe D. (1994) Radiation induction of immediate early genes: effectors of the radiation-stress response. *Int. J. Radiat. Oncol. Biol. Phys*. 30:229–34.
35. Ahmed MM. (2004) Regulation of radiation-induced apoptosis by early growth response-1 gene in solid tumors. *Curr. Cancer Drug Targets*. 4:43–52.
36. Anscher MS. (2010) Targeting the TGF-beta1 pathway to prevent normal tissue injury after cancer therapy. *Oncologist*. 15:350–9.
37. Boerma M, Wang J, Sridharan V, Herbert JM, Hauer-Jensen M. (2013) Pharmacological induction of transforming growth factor-beta1 in rat models enhances radiation injury in the intestine and the heart. *PLoS One*. 8:e70479.
38. Pohlers D, *et al*. (2009) TGF-beta and fibrosis in different organs - molecular pathway imprints. *Biochim. Biophys. Acta*. 1792:746–56.
39. Westbury CB, Yarnold JR. (2012) Radiation fibrosis—current clinical and therapeutic perspectives. *Clin. Oncol. (R. Coll. Radiol.)*. 24:657–72.
40. Imaizumi N, Monnier Y, Hegi M, Mirimanoff RO, Ruegg C. (2010) Radiotherapy suppresses angiogenesis in mice through TGF-betaRI/ALK5-dependent inhibition of endothelial cell sprouting. *PLoS One*. 5:e11084.
41. Martin M, Lefaix J, Delanian S. (2000) TGF-beta1 and radiation fibrosis: a master switch and a specific therapeutic target? *Int. J. Radiat. Oncol. Biol. Phys*. 47:277–90.
42. Akhurst RJ, Hata A. (2012) Targeting the TGFbeta signalling pathway in disease. *Nat. Rev. Drug. Discov*. 11:790–811.
43. Chai Y, *et al*. (2013) Radiation-induced non-targeted response in vivo: role of the TGFbeta-TGFBR1-COX-2 signalling pathway. *Br. J. Cancer*. 108:1106–12.
44. Biernacka A, Dobaczewski M, Frangogiannis NG. (2011) TGF-beta signaling in fibrosis. *Growth Factors*. 29:196–202.
45. Leask A, Abraham DJ. (2004) TGF-beta signaling and the fibrotic response. *FASEB J*. 18:816–827.
46. Hall BE, *et al*. (2010) Conditional overexpression of TGF-beta1 disrupts mouse salivary gland development and function. *Lab. Invest*. 90:543–55.
47. Bhattacharyya S, *et al*. (2011) Early growth response transcription factors: key mediators of fibrosis and novel targets for anti-fibrotic therapy. *Matrix Biol* .30:235–42.
48. Fang F, *et al*. (2011) The early growth response gene Egr2 (Alias Krox20) is a novel transcriptional target of transforming growth factor-beta that is up-regulated in systemic sclerosis and mediates profibrotic responses. *Am. J. Pathol*. 178:2077–90.

49. Wu M, *et al*. (2009) Essential roles for early growth response transcription factor Egr-1 in tissue fibrosis and wound healing. *Am. J. Pathol*. 175:1041–55.
50. Chen SJ, *et al*. (2006) The early-immediate gene EGR-1 is induced by transforming growth factor-beta and mediates stimulation of collagen gene expression. *J. Biol. Chem*. 281:21183–97.
51. Lai CF, *et al*. (2013) Cysteine-rich protein 61 plays a proinflammatory role in obstructive kidney fibrosis. *PLoS One*. 8:e56481.
52. Kular L, Pakradouni J, Kitabgi P, Laurent M, Martinerie C. (2011) The CCN family: a new class of inflammation modulators? *Biochimie*. 93:377–88.
53. Sweetwyne MT, Murphy-Ullrich JE. (2012) Thrombospondin1 in tissue repair and fibrosis: TGF-beta-dependent and independent mechanisms. *Matrix Biol*. 31:178–86.
54. Guarino M, Tosoni A, Nebuloni M. (2009) Direct contribution of epithelium to organ fibrosis: epithelial-mesenchymal transition. *Hum. Pathol*. 40:1365–76.
55. Kalluri R, Neilson EG. (2003) Epithelial-mesenchymal transition and its implications for fibrosis. *J. Clin. Invest*. 112:1776–84.
56. Moore BB, Hogaboam CM. (2008) Murine models of pulmonary fibrosis. *Am. J. Physiol. Lung Cell Mol. Physiol*. 294:L152–60.
57. Moen I, *et al*. (2009) Hyperoxic treatment induces mesenchymal-to-epithelial transition in a rat adenocarcinoma model. *PLoS One* 4:e6381.
58. Romero-Valdovinos M, *et al*. (2011) Keloid skin scars: the influence of hyperbaric oxygenation on fibroblast growth and on the expression of messenger RNA for insulin like growth factor and for transforming growth factor. *In Vitro Cell. Dev. Biol. Anim*. 47:421–4.
59. Borcek AO, *et al*. (2013) Hyperbaric oxygen in epidural fibrosis: is there a potential for treatment? *Turk. Neurosurg*. 23:607–10.
60. Celik B, Meydan AD, Kefeli M, Gulen EK, Okumus NO. (2010) The effects of hyperbaric oxygen treatment on the healing of tracheal anastomosis following irradiation in rats. *Thorac. Cardiovasc. Surg*. 58:481–5.
61. Khan M, *et al*. (2012) Oxygen cycling in conjunction with stem cell transplantation induces NOS3 expression leading to attenuation of fibrosis and improved cardiac function. *Cardiovasc. Res*. 93:89–99.
62. Kuran FD, Pekedis M, Yildiz H, Aydin F, Eliyatkin N. (2012) Effect of hyperbaric oxygen treatment on tendon healing after Achilles tendon repair: an experimental study on rats. *Acta. Orthop. Traumatol. Turc*. 46:293–300.
63. Li M, Jendrossek V, Belka C. (2007) The role of PDGF in radiation oncology. *Radiat. Oncol*. 2:5.
64. Brizel DM, *et al*. (1995) The mechanisms by which hyperbaric oxygen and carbogen improve tumour oxygenation. *Br. J. Cancer*. 72:1120–4.